International Journal of ENGINE RESEARCH

*Standard Article*

*International J of Engine Research*
1–15

DOI: 10.1177/1468087420923451
journals.sagepub.com/home/jer
SAGE

# Experimental investigations of mineral diesel/methanol-fueled reactivity controlled compression ignition engine operated at variable engine loads and premixed ratios

**Akhilendra Pratap Singh, Nikhil Sharma, Vikram Kumar and Avinash Kumar Agarwal**

## Abstract

Global warming and stringent emission norms have become the major concerns for the road transport sector globally, which has motivated researchers to explore advanced combustion technologies. Reactivity controlled compression ignition combustion technology has shown great potential to resolve these issues and deliver high brake thermal efficiency and emit ultra-low emissions of oxides of nitrogen and particulate simultaneously. In this experimental study, baseline compression ignition combustion mode and reactivity controlled compression ignition combustion mode experiments were performed in a single-cylinder research engine using mineral diesel as high-reactivity fuel and methanol as low-reactivity fuel. All experiments were carried out at constant engine speed at four engine loads (brake mean effective pressure: 1–4 bar). For efficient combustion and lower emissions, four premixed ratios ($r_p$ = 0, 0.25, 0.50, and 0.75) were tested to assess optimized premixed ratio at different engine loads. In these experiments, primary and secondary fuel injection parameters were maintained identical. Combustion results showed that reactivity controlled compression ignition combustion was more stable compared to compression ignition combustion and resulted in lesser knocking. Reactivity controlled compression ignition combustion delivered higher brake thermal efficiency and lower exhaust gas temperature and oxides of nitrogen emissions, especially at maximum engine loads. Addition of methanol as secondary fuel reduced particulate emissions. Particulate analyses depicted that reactivity controlled compression ignition combustion mode emitted significantly lower accumulation mode particles; however, emission of nucleation mode particles was slightly higher. A significant reduction in particulate mass emitted from reactivity controlled compression ignition combustion was another important finding of this study. Particulate number–mass distributions showed that increasing the premixed ratio of methanol led to a dominant reduction in particulate number concentration compared to particulate mass. Analysis for critical performance and emission characteristics suggested that optimization of the premixed ratio of methanol at each engine load should be done in order to achieve the best results in reactivity controlled compression ignition combustion mode.

**Keywords**

Reactivity controlled compression ignition, methanol, combustion, particulate matter

Date received: 18 February 2020; accepted: 9 April 2020

## Introduction

The development of clean and highly efficient internal combustion (IC) engines remains the most exciting research problem for IC engine developers/researchers. Compression ignition (CI) engines are the first choice as power plants in various sectors of the economy such as light-duty and heavy-duty vehicles for transport sectors, gensets for decentralized power generation in the

Engine Research Laboratory, Department of Mechanical Engineering, Indian Institute of Technology Kanpur, Kanpur, India

**Corresponding author:**
Avinash Kumar Agarwal, Engine Research Laboratory, Department of Mechanical Engineering, Indian Institute of Technology Kanpur, Kanpur 208016, India.
Email: akag@iitk.ac.in

energy sector, and agriculture sector.[1] Various technological advancements such as common rail direct injection (CRDI) and gasoline direct injection (GDI) have improved the overall engine efficiency and reduced harmful tailpipe emissions.[2] However, many of these contemporary technologies are unable to meet existing stringent emission norms independently. Therefore, use of exhaust gas after-treatment systems such as diesel oxidation catalysts (DOCs), diesel particulate filters (DPFs), selective catalytic reduction (SCR), lean oxide of nitrogen (NOx) traps, and three-way catalytic converters (TWCs) have been explored. These technologies have the potential to reduce engine emissions to meet prevailing emission norms. However, there are limitations such as system complexity, cost, and limited operating range, which restrict their application in a vast segment of road transport vehicles.[3]

Rapidly increasing fossil fuel consumption and associated environmental and health issues have gained global attention and motivated the energy sector policymakers to move toward alternative energy resources such as alcohols, biodiesel, and hydrogen. Primary alcohols (methanol, ethanol, and butanol) can be produced from renewable resources and have the potential to replace conventional petroleum-based fossil fuels.[4] Among these alcohols, methanol has excellent fuel properties such as high octane number (ON) and high latent heat of vaporization, which makes it suitable for applications in CI engines.[5] Recent experimental studies have demonstrated that the exhaust emitted by methanol-fueled engines is less toxic compared to conventional gasoline and diesel-fueled vehicles.[6–9] Previous experimental studies also showed that the use of alcohol with mineral diesel reduced carbon monoxide (CO), NOx, and particulate matter (PM) emissions, but slightly increased hydrocarbon (HC) emissions and brake-specific fuel consumption (BSFC).[9,10] Rakopoulos et al.[10] used different blends of butanol and mineral diesel in a CI engine and reported superior brake thermal efficiency (BTE) of butanol–diesel blend compared to conventional diesel combustion. Unfortunately, alcohol blending with mineral diesel cannot eliminate NOx–PM trade-off issue of the conventional diesel combustion.[11] Therefore, it becomes necessary to explore new, advanced combustion concepts such as low temperature combustion (LTC) that can be applied to all segments of IC engines without NOx–PM trade-off, and has potential to be fuelled by alternative fuels.[12]

In the last two decades, many advanced combustion concepts/technologies have been developed, among which, homogeneous charge compression ignition (HCCI), premixed charge compression ignition (PCCI), and so on are some of the important ones, which have the potential to reduce both the NOx and the PM emissions simultaneously, without affecting the engine performance adversely.[13,14] However, these combustion techniques suffer in the manner of combustion control, which limits the application of these techniques at higher engine load conditions. Several researchers explored combustion mode switching between different engine combustion modes and developed prototype engines, which can be operated up to full engine load conditions.[15,16] However, the commercialization of these technologies has not happened so far since these technologies have not matured enough. In the last few years, a new derivative of LTC named "Reactivity controlled compression ignition" (RCCI) has been developed for commercial engines. Initially, RCCI combustion was explored by Kokjohn and colleagues,[17–19] wherein they used two different fuels, namely, a high-reactivity fuel (HRF) and a low-reactivity fuel (LRF) in a CI engine. The combination of two test fuels created reactivity stratification in the engine combustion chamber. In RCCI combustion, HRF (primary fuels) was taken to be a high cetane fuel such as mineral diesel or biodiesel. LRF (secondary fuels) was taken to be a low-cetane fuel such as gasoline, alcohols, or compressed natural gas (CNG). The LRF was injected in the intake manifold, where it mixed with the intake air. This premixed charge was then supplied to the combustion chamber. During the compression stroke, this premixed charge homogenized and then HRF was directly injected into the combustion chamber. In RCCI combustion, reactivity gradient is the key parameter, which controls the combustion parameters such as the start of combustion (SoC), combustion phasing (CP), end of combustion (EoC), pressure rise rate (PRR), and heat release rate (HRR).[20]

Kokjohn et al.[19] and Zhou et al.[20] used gasoline (research octane number (RON) = 95.6) and mineral diesel (cetane number (CN) = 46.1) pair for achieving RCCI combustion and reported that the premixed ratio of LRF was the most important parameter for controlling the CP. In an optical engine investigation, it was reported that RCCI combustion was similar to HCCI combustion and combustion was controlled chemically[19] even if a significant amount of HRF was directly injected into the combustion chamber. Curran et al.[21] achieved RCCI combustion in a multi-cylinder engine and reported a significant simultaneous reduction in NOx and PM emissions. In another study carried out in a multi-cylinder light-duty engine, they claimed that RCCI combustion resulted in relatively superior BTE compared to conventional CI combustion.[22] Dempsey and Reitz[23] simulated RCCI combustion at high engine loads (indicated mean effective pressure (IMEP): 23 bar) using an ultra-low compression ratio and reported that RCCI was capable of catering to the full-load application without any reduction in BTE compared to CI combustion. They also reported a significant reduction in PM and NOx emissions.[23] Splitter et al.[24] demonstrated that comparable RCCI results were possible using a single fuel (directly injected fuel with a cetane improver, which makes it more reactive). A few researchers also carried out simulation studies for RCCI combustion and explored the suitability of different control parameters such as fuel pair, fuel

injection parameters, exhaust gas recirculation (EGR), and intake valve closing (IVC) timings on the RCCI combustion control.[25,26] Zheng et al.[27] carried out RCCI experiments to investigate the effect of butanol blending with mineral diesel on both CI combustion and LTC. They reported that the blending of butanol with mineral diesel improved the BTE at a certain EGR range. They found that PM emissions from LTC engine decreased with increasing blending ratio of butanol in the mineral diesel. Splitter et al.[24] performed RCCI combustion experiments using E85 as LRF and mineral diesel as HRF, and reported ~59% gross indicated thermal efficiency (ITE). Hanson et al.[28] also performed similar experiments using E20/mineral diesel fuel pair. They reported that the use of ethanol–gasoline blend as LRF resulted in lower PRR compared to gasoline, which extended the RCCI combustion operating regime envelope from a maximum brake mean effective pressure (BMEP) of 8–10 bar.

Many researchers suggested that methanol is another suitable LRF for RCCI combustion. Due to the higher RON of methanol (RON = 109) compared to gasoline (RON = 95.6), the reactivity difference between methanol/diesel fuel pair was higher compared to gasoline/diesel fuel pair.[18,29] This led to more efficient combustion and superior control over the combustion compared to other test fuel pairs. Dempsey et al.[30] carried out RCCI experiments using methanol as the LRF and mineral diesel with Cetane Improver as the HRF. They emphasized on start of injection (SoI) timing of HRF and the premixed ratio of LRF as "sensitive parameters," which affected the ignition timing. They reported that HRR shape can be effectively controlled by optimizing these parameters, which resulted in smoother RCCI combustion. Li et al.[31] also used a multi-dimensional model to investigate the effect of methanol fraction, SoI timing of HRF, and initial temperature on engine performance and emission characteristics. They also reported that methanol/diesel RCCI combustion improved engine performance and decreased the exhaust emissions significantly.

Although several studies have been performed to investigate the combustion, performance, and emission characteristics of methanol/diesel fuel pair, however, most of them are simulation-based studies. Very limited experimental studies are available in the open literature, in which detailed PM emission characteristics of RCCI combustion have been reported.[11,12,19,30] In this study, RCCI combustion investigations were carried out using methanol as the LRF and mineral diesel as the HRF. Previous studies exhibited that the amount of LRF depends on the engine load; therefore, this study aims to explore the maximum limit of energy replacement of HRF using LRF at varying engine loads. The experiments were performed at different engine loads (1, 2, 3, and 4 bar BMEP) and different premixed ratios ($r_p$ = 0.25, 0.50, and 0.75) of methanol. This study experimentally explores all aspects of RCCI combustion, including combustion, performance, emission, and particulate characteristics. Qualitative correlations between particulate characteristics and performance and emission characteristics are the innovative aspects of this study. This study also explores the optimum premixed ratios at different engine loads to achieve higher BTE along with lower NOx and PM emissions. This provides valuable information for adaptation of RCCI combustion in production-grade engines and it has not been reported in the previous studies.

## Experimental setup

For this experimental study, a single-cylinder research engine (AVL; 5402) was used, which can operate in both combustion modes, that is, RCCI as well as CI, depending on the fuel injection strategies and EGR. The schematic of the experimental setup is shown in Figure 1.

This test engine is a single-cylinder version of a multi-cylinder commercial diesel engine, equipped with a CRDI system, and it can have up to four injections in an engine cycle (two pre-injections, one main, and one post-injection). The technical specifications of the test engine are given in Table 1.

To perform the experiments under controlled engine conditions (speed and load), a transient (alternating current (AC)) dynamometer (Wittur Electric Drives; 2SB 3) was used, which was capable of motoring the engine up to 3000 r/min. For controlling the fuel injection parameters of the HRF, an engine management system (EMS) was used in an open-loop configuration. The EMS was a combination of an electronic control unit (ECU), a communication interface (ETAS; ETK 7.1 Emulator probe), and a commercial software tool for automotive calibration (ETAS; INCA), which effectively controls the fuel injection parameters such as fuel injection pressure (FIP), SoI timing, and injection strategy. For the LRF induction, a low-pressure fuel injection system was used, which consisted of an electric PFI fuel pump, a fuel tank, a fuel accumulator, a port fuel injection (PFI) fuel injector (Denso; 1500M844M1), and an injector control circuit. The fuel injection parameters were controlled by a 12 V transistor–transistor logic (TTL) pulse given by the injector control circuit, which controlled the injector solenoid. Other important parameters of the injector driver circuit are given in Table 2.

To avoid the effects of variations in fuel temperature and lubricating oil temperature during the experiments, dedicated fuel conditioning system (AVL; 553) and lubrication oil conditioning system (Yantrashilpa; YS4312) were used. In this study, fuel temperature and lubricating oil temperature were maintained constant at 25 °C and 90 °C, respectively. For measurement of fuel mass flow rate and air mass flow rate, a fuel-metering unit (AVL; 733S) and an inlet airflow rate measurement unit (ABB Automation; Sensy-flow P) were installed in the experimental setup. A coolant conditioning system

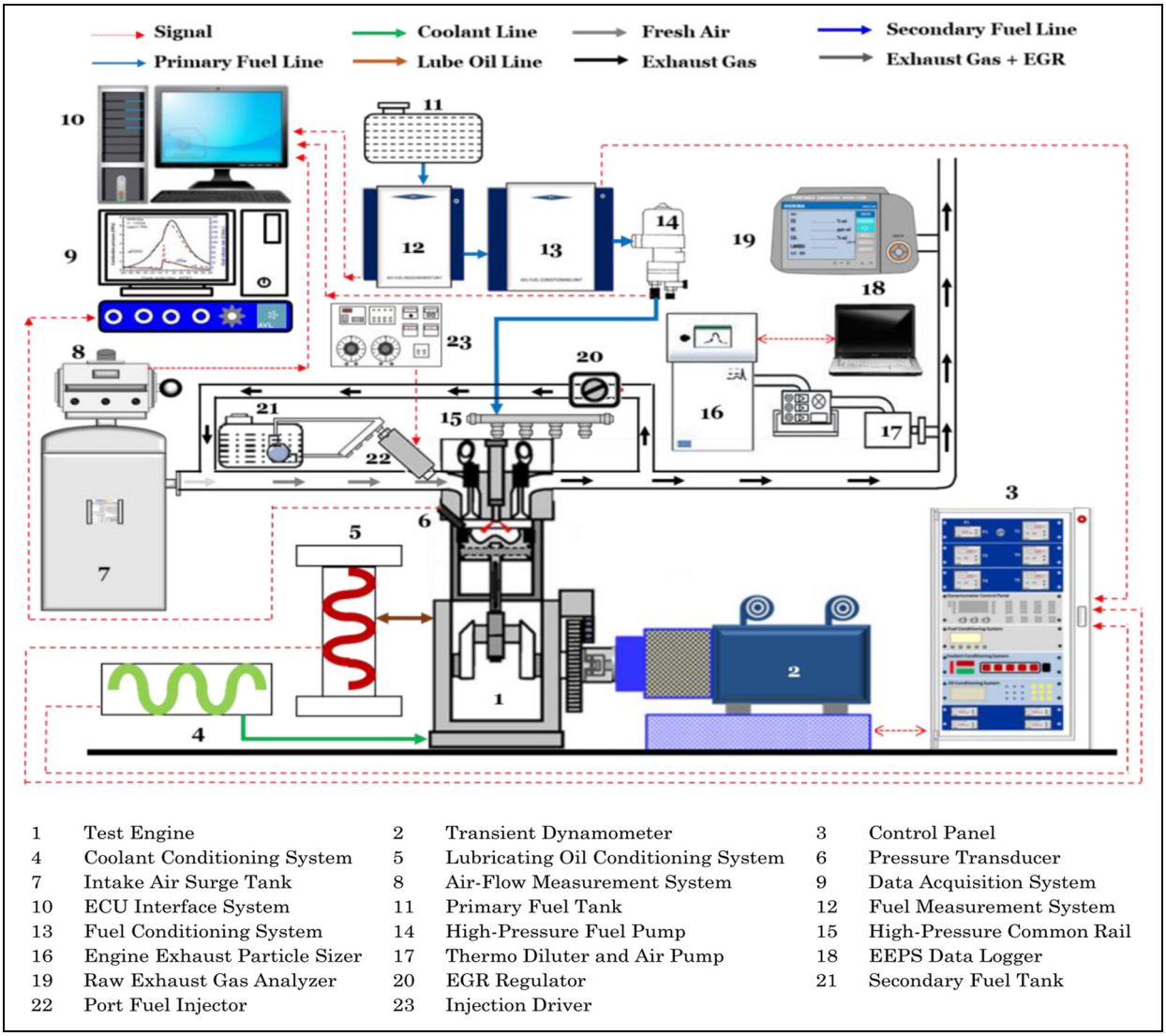


**Figure 1.** Schematic of the experimental setup.

**Table 1.** Specifications of the test engine.

| | |
|---|---|
| Engine make/model | AVL/5402 |
| Number of cylinder/s | One |
| Cylinder bore/stroke | 85/90 mm |
| Swept volume | 510.7 cc |
| Compression ratio | 17.1 |
| Inlet ports | Tangential and swirl inlet port |
| Nominal swirl ratio | 1.78 |
| Maximum power output | 6 kW |
| Rated speed | 4200 r/min |
| Fuel injection pressure | 200–1400 bar |
| Fuel injection system | Common rail direct injection |
| High-pressure system | BOSCH Common Rail CP4.1 |
| Engine management system | AVL-RPEMS + BOSCH ETK7 |
| Valves per cylinder | Four (two inlets and two exhaust) |

**Table 2.** Specifications of the injector driver circuit.

| Characteristics | Specifications |
|---|---|
| Input signal | 5.0 V DC pulse |
| Output signal | 12 V square pulse |
| Power supply | 12 V DC |
| Minimum pulse duration | 1 ms |
| Maximum pulse duration | 35 ms |
| Step size | 0.01 ms |
| Maximum injection lag | 12 ms |

DC: direct current.

(Yantrashilpa; YS4027) was used to maintain the temperature of the coolant at 60 °C. In order to control the combustion, a fraction of exhaust gas was mixed with fresh intake air as EGR. The EGR rate was regulated by an EGR control valve, which was installed in the EGR line. For measurement of temperatures such as exhaust gas temperature (EGT), intake air temperature, coolant inlet, and outlet temperatures, thermocouples were installed at relevant locations in the experimental setup. For in-cylinder combustion data acquisition, a water-cooled piezoelectric pressure transducer (AVL;

**Table 3.** Technical specifications of exhaust gas emission analyzer.[32]

| Species | Measurement principle | Range | Repeatability |
|---|---|---|---|
| CO | Non-dispersive infrared (NDIR) | 0%–10% | 0.01% |
| HC | | 0–20,000 ppm | 3.3 ppm |
| $CO_2$ | | 0%–20% | 0.17% |
| NOx | NO sensor | 0–5000 ppm | 5 ppm |

CO: carbon monoxide; HC: hydrocarbon; $CO_2$: carbon dioxide; NOx: oxide of nitrogen.

QC34C) was mounted flush with the cylinder head. The sensitivity of the pressure transducer was 23.09 pC/bar and it could measure in-cylinder pressures up to 250 bar. An optical shaft encoder (AVL; 365C) was installed to record the position of the crankshaft. All low-voltage signals were supplied to a high-speed data acquisition system (AVL; IndiMicro), after signal amplification using a charge amplifier (AVL) for data acquisition and analysis.

For engine exhaust and particulate characterization, an exhaust gas emission analyzer (Horiba; 584L) and an Engine Exhaust Particle Sizer (EEPS) spectrometer (TSI Inc.; 3090) were used, respectively. Gaseous emission analyzer was capable of measuring different gaseous exhaust species such as CO, HC, NOx, and $CO_2$. Other technical details of the gaseous emission analyzer are given in Table 3.

EEPS was used to measure the number–size distribution of particles emitted by the engine. This instrument is capable of measuring up to a maximum concentration of $\#10^8$ particles/cm$^3$ in the engine exhaust, which can vary in a wide size range (from 5.6 to 560 nm). EEPS is capable of measuring higher particle concentrations using a rotating disk thermo-diluter (Matter Engineering; MD19-2E), which dilutes the exhaust gas to bring the particulate concentration within the measuring range of EEPS. In this system, particles get charged based on their size by the ions produced by an electrical diffusion charger. These charged particles then pass through an electric field, which repels these particles toward the electrometer rings. These sensitive electrometers rings collect the charge of these particles and provide information about their numbers and size distributions. Other important details of EEPS and detailed working principle can be seen in our previous publications.[33,34]

Experiments were performed at constant engine speed (1500 r/min) and four engine loads (1, 2, 3, and 4 bar BMEP) in both combustion modes, that is, RCCI combustion mode, and baseline CI combustion mode. Due to excessive knocking during baseline CI combustion and RCCI combustion at lower $r_p$, the experiments were limited up to 4 bar BMEP only. The premixed ratio ($r_p$) is defined as the ratio of port-injected fuel energy to the total fuel energy injected. The following formula is used for calculations

$$r_p = \frac{m.(LHV)_s}{M.(LHV)_p + m.(LHV)_s}$$

where $M$ and $m$ are the mass flow rates of primary and secondary fuels respectively, and $LHV$ is the lower heating value of the respective fuels. The subscript $p$ and $s$ represent the primary and secondary fuels, respectively. For RCCI experiments, three premixed ratios of methanol were used ($r_p$ = 0.25, 0.50, and 0.75); however, for baseline CI combustion ($r_p$ = 0), i.e., no methanol was injected in the intake port. The premixed ratios of methanol were decided based on energy replacement targeted. In all experiments, mineral diesel was injected at 500 bar FIP and SoI timing was maintained constant at 17 °CA before top dead center (bTDC). During both CI as well as RCCI modes, 15% EGR was used to control the combustion. All parameters related to both combustion modes, namely, RCCI and CI, are given in Figure 2.

Important test fuel properties such as $LHV$, kinematic viscosity, and density were measured using a bomb calorimeter (Parr; 6200), a kinematic viscometer (Stanhope-Seta; 83541-3), and a portable density meter (Kyoto Electronics; DA130N), respectively. These important properties of the test fuels are given in Table 4.

Using in-cylinder pressure data, mass fraction burn (MFB) analysis was also performed, using the "Rassweiler and Withrow" method[35]

$$(\Delta p_c) = p_i - p_{i-1}\left(\frac{V_{i-1}}{V_i}\right)^{\gamma}$$

where $\Delta p_c$ represents the change in the in-cylinder pressure and $\gamma$ is the polytropic exponent

$$\frac{m_{b(i)}}{m_{b(total)}} = \frac{\sum_{j=0}^{i} \Delta(p_c)_j}{\sum_{j=0}^{N} \Delta(p_c)_j}$$

Here it is assumed that sample 0 is between IVC and SoC and sample N represents the completion of combustion. Using MFB analysis, three important parameters, namely, SoC, CP and, combustion duration (CD) were calculated. Crank angle (CA) position corresponding to 10% cumulative heat release (CHR) ($CA_{10}$) represents the SoC. CA position corresponding to 50% CHR ($CA_{50}$) represents the CP, which is a measure of overall combustion during an engine cycle. For stable RCCI combustion, CP is the most critical parameter that needs to be optimized for higher BTE and reduced emissions. It has been reported that too advanced CP results in high PRR and knocking. However, too retarded CP leads to higher HC and CO emissions due to incomplete combustion.[36] CD is another important parameter, which is the crank angle

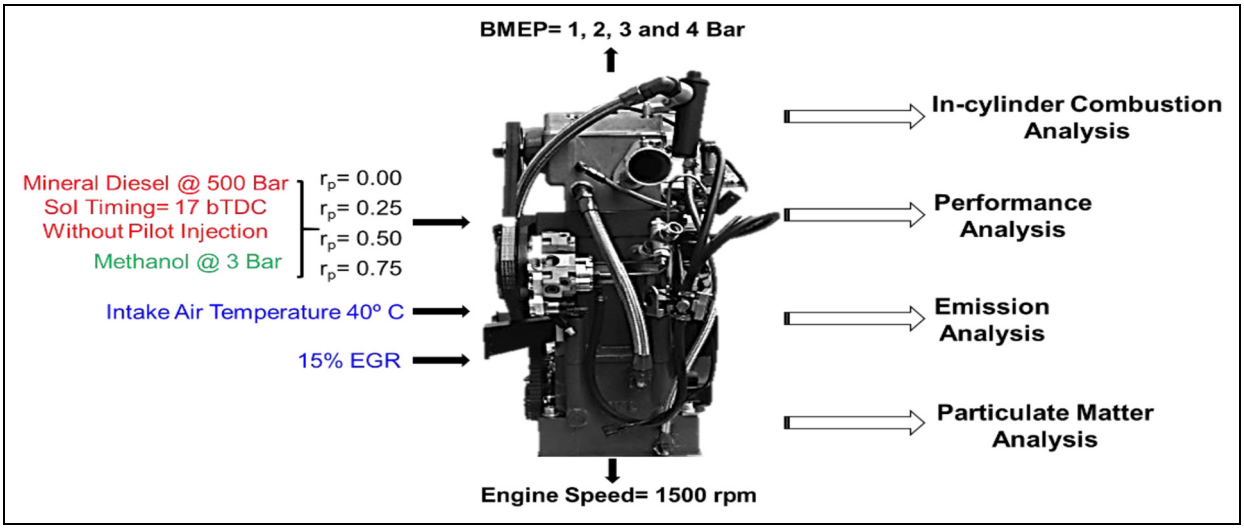


**Figure 2.** Experimental methodology.

**Table 4.** Properties of test fuels.

| Test fuel | Calorific value (MJ/kg) | Kinematic viscosity ($mm^2/s$) at 40 °C | Density ($g/cm^3$) at 30 °C |
|---|---|---|---|
| Diesel | 44.26 | 2.96 | 0.837 |
| Methanol | 19.76 | 0.798 | 0.783 |

degree (CAD) difference between the EoC (CA position corresponding to 90% CHR ($CA_{90}$)) and SoC (CA position corresponding to 10% CHR ($CA_{10}$)).

In these experiments, all measurements were done after thermal stabilization of the test-engine in order to reduce the experimental errors. To reduce the measurement errors, experiments were performed thrice and the average of these was reported as the data set. In this study, root-of-the-sum-of-the-squares (RSS) concept was used for uncertainty analysis, in which all uncertainties such as precision, bias, calibration, and measurement uncertainties were considered. Uncertainty data provided by the emission measurement systems have been also included in the error measurement.

## Results and discussion

In this study, a single-cylinder engine was modified to operate in RCCI combustion mode using mineral diesel as primary (high-reactivity) fuel and methanol as secondary (low-reactivity) fuel (Figure 2). For RCCI investigations, in-cylinder combustion analysis, performance and emission analysis, and detailed particulate characterizations were performed. In all sections, results are explained for two load ranges, namely, low engine load (BMEP $<$ 2 bar) and medium engine load (BMEP $>$ 2 bar) conditions.

### *Combustion investigations*

For combustion analysis, in-cylinder pressure and CA signals were acquired as input from piezoelectric pressure transducer and shaft encoder, respectively. In order to avoid the effect of cyclic variations, combustion data of 250 consecutive engine cycles were acquired and the average data set of these 250 cycles was used for further analysis. Combustion investigations included in-cylinder pressure and HRR variations w.r.t. engine load (Figure 3), MFB analysis (Figure 4), and knocking and noise analyses (Figure 5).

Figure 3 shows the in-cylinder pressure variations (solid lines) and HRR (dotted lines) variations w.r.t. CAD at varying engine loads for four premixed ratios. At all engine loads, in-cylinder pressure variations during combustion was shown with motoring pressure variations in order to examine the effect of methanol addition on the in-cylinder conditions, the SoC, and so on. At all engine loads, separation of in-cylinder pressure curves from the motoring curve shows the SoC. At lower $r_p$, increasing engine load advanced the SoC for both baseline CI combustion mode and RCCI combustion mode. Relatively higher in-cylinder temperature due to the presence of no/low methanol fraction may be the reason for this trend, which improved fuel–air mixture chemical kinetics. However, at higher $r_p$, this trend was not followed strictly due to presence of a relatively higher quantity of methanol in the combustion chamber, which resulted in a dominant cooling effect and reduced the overall fuel–air mixture reactivity. The effect of methanol addition on combustion was clearly visible at all engine loads. Increasing $r_p$ retarded the combustion due to dominant methanol–air chemical kinetics. At lower engine loads (up to BMEP = 2 bar), increasing premixed ratio reduced the peak in-cylinder pressure; however, at medium engine loads (BMEP $>$ 2 bar), this effect was visible only for higher

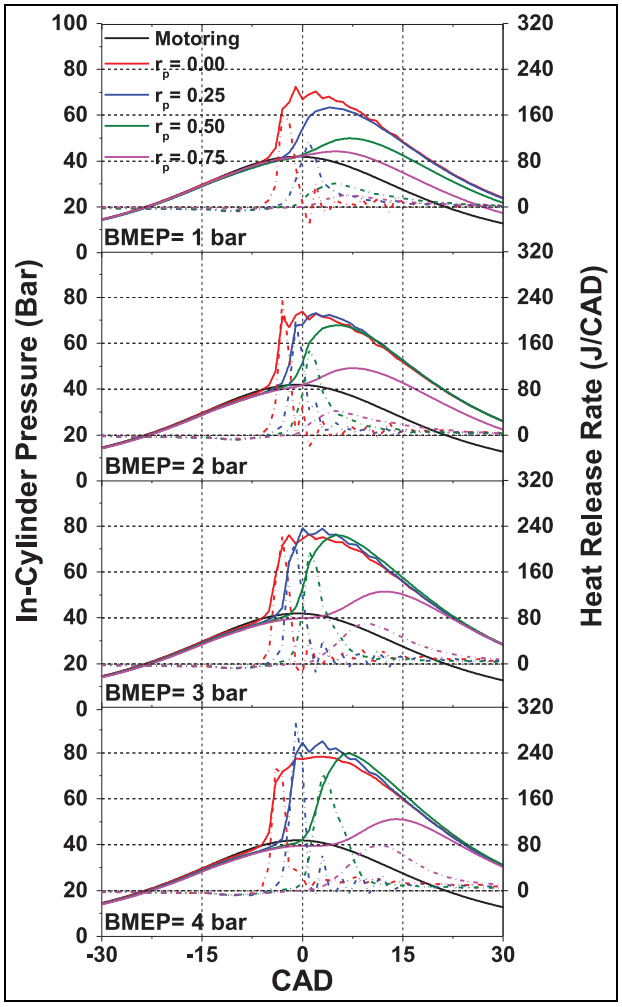


**Figure 3.** In-cylinder pressure and HRR variations w.r.t. CAD in RCCI combustion mode at different engine loads and premixed ratios.

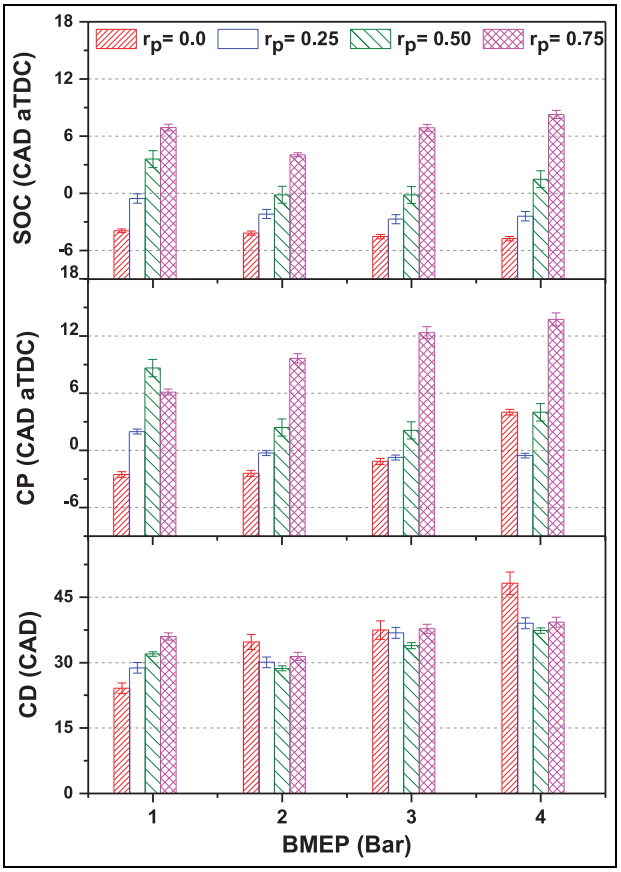


**Figure 4.** Start of combustion, combustion phasing, and combustion duration in RCCI combustion mode at different engine loads and premixed ratios.

premixed ratios ($r_p = 0.75$). This may be due to the temperature dependence of the combustion kinetics of the methanol–air mixture.[31] In some conditions (especially for CI combustion), the knocking was observed; however, increasing $r_p$ resulted in relatively smoother combustion. Among all engine conditions tested, it was found that optimum $r_p$ for methanol varied with varying engine loads. At lower engine loads, lower $r_p$ was better; whereas higher $r_p$ was suitable to be used at medium engine loads.

HRR analysis is another important parameter, which provides vital information about combustion. HRR is calculated using the "first law of thermodynamics."[37] Similar to in-cylinder pressure curves, HRR curves also retarded with increasing $r_p$ (Figure 3). Peak HRR increased with increasing engine load and decreased with increasing $r_p$. Relative dominance of increasing engine load and methanol addition can be seen in HRR curves of medium load and $r_p$. Significantly lower HRR at $r_p = 0.75$ was an important observation, which represented the highest energy replacement limit by methanol. Width of HRR curve is an indirect measure of CD, which shows that increasing engine load shortens the CD; however, increasing $r_p$ leads to relatively longer CD.

Figure 4 shows that the SoC is an important parameter in RCCI combustion mode, which is affected by several variables such as engine operating conditions, fuel properties, and inlet air temperature. Experiments showed that increasing engine load resulted in slightly earlier SoC due to relatively more intense in-cylinder conditions at medium engine load. This trend was observed in CI combustion mode as well as in the RCCI combustion mode at lower $r_p$. However, at higher $r_p$ ($r_p = 0.50$ and 0.75), SoC was significantly retarded at medium engine loads. Dominating effect of LRF may be the main reason for this trend, which resulted in a longer ignition delay compared to lower engine loads. At all engine loads, increasing $r_p$ resulted in retarded SoC. This is the advantage of RCCI combustion mode, in which the relative proportion of LRF and HRF controls the combustion, as also indicated by several other researchers.[18,19,30]

CP variation at different engine loads and $r_p$ showed an interesting trend. For CI and RCCI combustion modes at higher $r_p$, CP retarded at medium engine

loads; however, RCCI combustion mode at lower $r_p$ resulted in advanced CP at medium engine loads. For CI combustion mode, the presence of larger fuel quantity was the main reason for retarded CP at medium engine loads. In RCCI combustion mode at $r_p = 0.75$, slower fuel–air combustion kinetics led to delayed CP. CP in RCCI combustion mode at lower $r_p = 0.25$ was mainly controlled by the HRF, which resulted in faster combustion of premixed LRF present in the combustion chamber. RCCI combustion at $r_p = 0.50$ showed a mixed trend, in which LRF dominated at lower engine loads, resulting in advanced CP; however, the presence of larger fuel quantity dominated at medium engine loads, leading to delayed CP. Similar to SoC and CP, the CD also followed the same trend and a trade-off between fuel reactivities was clearly observed. CD in CI combustion mode and RCCI combustion mode at lower $r_p$ was relatively higher at medium engine loads. The presence of relatively larger fuel quantity at medium engine load was the main reason for longer CD. In both CI as well as RCCI combustion modes at lower $r_p$, a large fraction of fuel burns during the "diffusion" (slower) combustion phase, which extends the CD. However, CD in RCCI combustion mode at higher $r_p$ showed a different trend: CD first decreased and then increased with increasing engine load. Relatively faster combustion of premixed LRF in presence of HRF may be a possible reason for such a trend, which inhibited due to dominant fuel–air combustion kinetics of LRF at medium engine loads. Comparison of CD in CI and RCCI combustion modes showed a mixed trend. At very low engine load (BMEP = 1 bar), RCCI combustion mode showed longer CD, which increased with increasing $r_p$. However, at medium engine loads (BMEP > 1 bar), RCCI combustion mode showed relatively shorter CD compared to CI combustion mode, which did not change significantly with changing $r_p$.

Knocking (knock integral (KI)) analysis and combustion noise analysis were also performed for both CI as well as RCCI combustion modes at different engine loads and $r_p$. Both KI and combustion noise were affected by maximum PRR ($R_{max}$); therefore, $R_{max}$ is also reported along with these parameters in Figure 5.

At lower engine loads (BMEP = 1–2 bar), CI combustion mode resulted in higher $R_{max}$ compared to RCCI combustion mode at all $r_p$. However, at medium engine loads (BMEP = 3–4 bar), RCCI combustion mode at $r_p = 0.25$ resulted in slightly higher $R_{max}$ compared to CI combustion mode and RCCI combustion mode at other values of $r_p$. At medium engine loads, the contribution of OH radicals generated from methanol combustion may be a possible reason for this trend, which dominated in the fuel–air combustion kinetics.[38] However, at operating conditions having lower engine loads and higher $r_p$, slower reactivity of LRF dominated due to the formation of more stable $H_2O_2$ radicals at lower in-cylinder temperatures.[38] At all engine loads, RCCI combustion at $r_p = 0.75$ showed

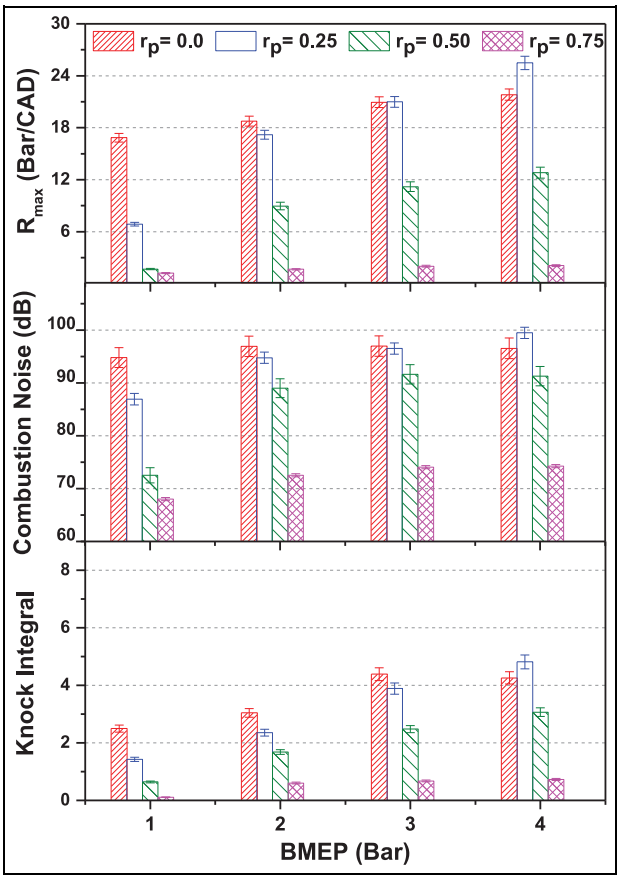


**Figure 5.** Maximum rate of pressure rise, combustion noise, and knock integral in RCCI combustion mode at different engine loads and premixed ratios.

significantly lower $R_{max}$, which did not change with increasing engine load. This is also visible in the in-cylinder pressure and HRR curves of RCCI combustion at $r_p = 0.75$ (Figure 3). Combustion noise is yet another parameter, which gives a good comparison of combustion stability between CI and RCCI combustion modes. Combustion noise was calculated from the measured in-cylinder pressure signals.[39] For both combustion modes, combustion noise increased with increasing engine load, which is similar to $R_{max}$. Combustion noise in CI combustion mode was relatively higher compared to RCCI combustion mode (except BMEP = 4 bar at $r_p = 0.25$). This is another advantage of RCCI combustion mode, which leads to relatively smoother combustion compared to CI combustion mode. With increasing $r_p$, combustion noise reduced, which showed the dominant contribution of LRF. KI is integral of superimposed rectified knock oscillations above the threshold limit. KI gives quantitative information about the combustion knock intensity. KI followed a similar trend as that of $R_{max}$ and the combustion noise. For both combustion modes, KI increased with increasing engine load. At all engine loads, KI of CI combustion mode was higher compared to RCCI combustion mode, which reduced with increasing $r_p$ in case of RCCI combustion. Similar to $R_{max}$, RCCI combustion at

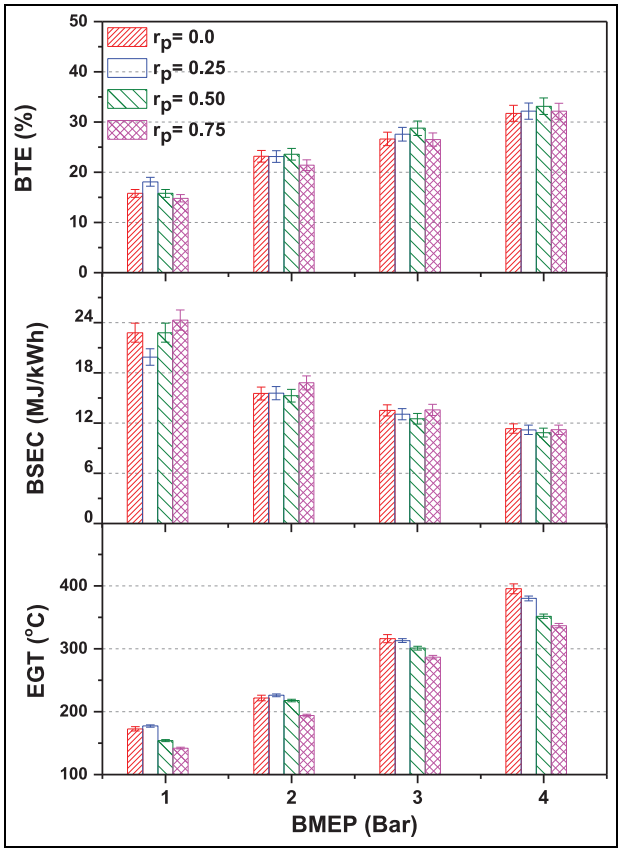


**Figure 6.** BTE, BSFC, and EGT in RCCI combustion mode at different engine loads and premixed ratios.

BMEP = 4 bar at $r_p = 0.25$ resulted in slightly higher KI compared to CI combustion mode and RCCI combustion mode at other values of $r_p$. Significant contribution of OH radicals generated from methanol combustion was the main reason for this trend, which became more dominant in presence of higher in-cylinder temperature at higher engine loads. Combined effect of these two factors, resulted in slightly different trend of $R_{max}$, combustion noise and KI at BMEP = 4 bar and $r_p = 0.75$.

## *Performance and emission investigations*

Figure 6 shows the performance characteristics of CI and RCCI combustion modes at different engine loads and $r_p$. Performance investigations included BTE and brake-specific energy consumption (BSEC), which were calculated using fuel consumption rates of both, primary and secondary fuels and the engine power output. EGT was also presented here as a performance parameter because it is a qualitative measure of in-cylinder combustion.[40]

Figure 6 shows that in both CI as well as RCCI combustion modes, BTE increased with increasing engine load. This is well-established for CI combustion mode and is also followed by the RCCI combustion mode. At medium engine loads, combined effect of higher mechanical efficiency and relatively superior combustion in presence of intense in-cylinder conditions (relatively higher in-cylinder temperature and pressure) resulted in higher power output. At all engine loads, BTE of RCCI combustion mode was comparable/or superior compared to CI combustion mode. This is an important observation of this study. At all engine loads, BTE trends showed slight reduction at higher $r_p$; however, variation in BTE at different $r_p$ was not significant. At lower engine loads, RCCI combustion at lower $r_p$ showed higher BTE; however, at medium engine loads, improved BTE was observed for higher $r_p$. Addition of methanol in the fuel pair affected the RCCI combustion mode in two ways. First, lower reactivity of methanol improved the CP at all engine loads. Second, the presence of fuel oxygen led to more complete combustion, which increased the BTE, especially at medium engine loads.[41] Dempsey and Reitz[23] also carried out RCCI experiments at high engine loads and reported that RCCI combustion exhibited better engine performance at higher engine loads. A strong relation of BTE with engine load and $r_p$ was another important finding of this study, which depicted that the engine performance could be maximized by optimization of $r_p$ at different engine loads. BSEC followed a reverse trend of BTE. BSEC reduced with increasing engine load. BSEC of RCCI combustion mode at lower $r_p$ was slightly lower compared to CI combustion, which slightly increased at higher $r_p$. Similar to BTE, EGT also increased with increasing engine load. A relatively larger fuel quantity injected in the port as well as directly into the combustion chamber was the main reason for higher EGT at higher engine loads. At all engine loads, EGT of CI combustion mode was relatively higher compared to RCCI combustion mode. This was mainly due to three factors, namely: (1) EGR effect, (2) domination of LRF, and (3) higher latent heat of vaporization of methanol. In RCCI combustion mode, recirculated exhaust gas absorbed a fraction of energy generated during combustion, which reduced the EGT. Due to the induction of methanol as LRF, combustion intensity reduced and a significant fraction of energy was absorbed in the vaporization of methanol, leading to relatively lower EGT. At all engine loads, EGT reduced with increasing $r_p$. The presence of larger methanol quantity was the main reason for this behavior, which hampered fuel–air combustion kinetics and absorbed a significant amount of latent heat for vaporization. At lower BMEP (1–2 bar), RCCI combustion mode at $r_p = 0.25$ resulted in slightly higher EGT compared to CI combustion mode. Improvement of combustion characteristics due to the presence of a smaller methanol quantity was the main reason for this.

Figure 7 shows the comparison of emission characteristics of CI and RCCI combustion modes at different engine loads and $r_p$. Emission investigations included measurements of CO, HC, and NOx. Raw emission concentrations measured for these pollutant species

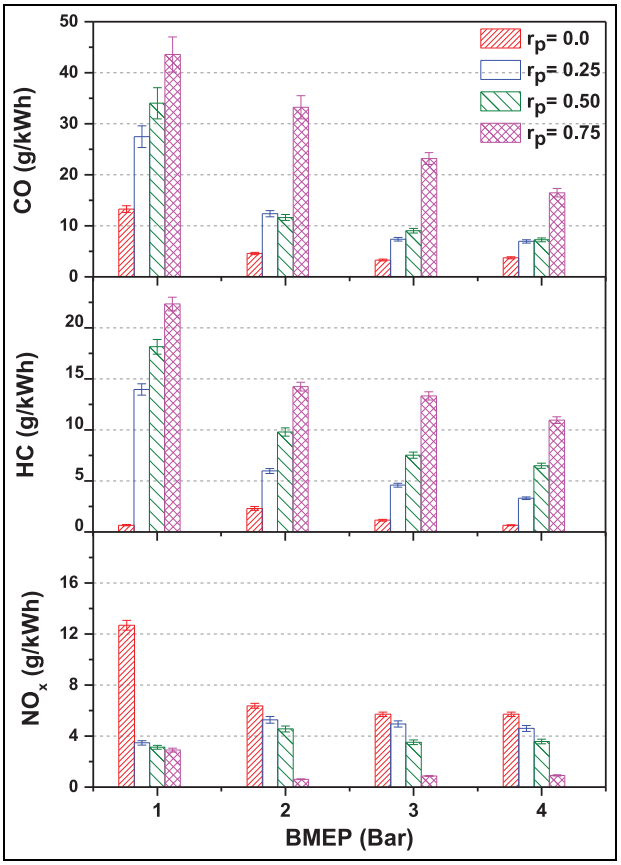


**Figure 7.** Mass emissions of CO, HC, and NOx in RCCI combustion mode at different engine loads and premixed ratios.

were converted into mass emissions (g/kWh) using standard methodology.[42]

CO is emitted due to incomplete combustion when the oxidation of CO into $CO_2$ does not get completed. Results showed that brake-specific CO emission decreased with increasing engine load. At lower engine loads, the in-cylinder temperature was low, which inhibited complete oxidation of CO into $CO_2$. At all engine loads, RCCI combustion mode emitted significantly higher CO compared to CI combustion mode. Lower in-cylinder temperature due to slower fuel–air chemical kinetics and higher latent heat of vaporization of methanol were the prime reasons for this. With increasing $r_p$, CO emission also increased and maximum CO was observed at $r_p = 0.75$. At higher engine loads (BMEP $>$ 1 bar), difference between CO emissions at $r_p = 0.25$ and 0.50 was negligible. HC emissions are emitted by the engines due to incomplete combustion of fuel, pyrolysis of lubricating oil, and flame quenching near the combustion chamber walls. Fuel trapped in the crevices also contributes significantly to the HC emissions, especially in the RCCI combustion mode. HC emissions followed a similar trend as that of CO. HC emissions reduced upon increasing engine load. HC emissions from RCCI combustion mode were significantly higher compared to CI combustion mode. Fuel trapped in the crevices contributed significantly to HC emissions in the RCCI combustion mode, especially at higher $r_p$. The relatively lower in-cylinder temperature may be another possible reason for the higher HC emissions from RCCI combustion mode. At all engine loads, HC emissions increased with increasing $r_p$. NOx were another important emissions, whose formation depends on three parameters, namely, peak in-cylinder temperature, presence of oxygen, and time availability for formation reactions.[35] In CI combustion mode, brake-specific NOx (BSNOx) emissions decreased with increasing engine load; however, in RCCI combustion mode, BSNOx emissions showed a rather random pattern. Relative dominance between peak in-cylinder temperature and contribution of fuel-bound oxygen during combustion were the main reasons for such variations in BSNOx emissions in RCCI combustion mode. For RCCI combustion mode, at lower $r_p$, BSNOx emissions first increased and then decreased with increasing engine load. Up to 2 bar BMEP, increasing engine load resulted in higher NOx emissions due to increasing in-cylinder temperature; however, at medium engine loads (at 3 and 4 bar BMEP), NOx emissions from RCCI combustion showed slight reduction. Dominant premixed phase combustion due to relatively faster fuel–air combustion kinetics may be a possible reason for lower NOx emissions at medium engine loads, which provides relatively lesser time for NOx formation in RCCI combustion mode at medium engine loads. At all engine loads, CI combustion mode emitted relative higher BSNOx compared to RCCI combustion mode. Relatively lower peak in-cylinder temperature due to slower fuel–air combustion kinetics in RCCI combustion mode and the presence of EGR were the main reasons for this. At all engine loads, increasing $r_p$ resulted in relatively lower BSNOx emissions. At higher $r_p$, combined effect of dominant premixed combustion phase and greater in-cylinder charge cooling due to the presence of larger methanol quantity in the combustion chamber resulted in lower NOx formation. These findings were in agreement with previous results reported by Li et al.[31]

Figure 8 shows a correlation between the performance and emission parameters. The main objective of this analysis was to optimize the $r_p$ at each engine load so that the maximum BTE could be achieved along with lower emissions. The inclination of curves toward the $x$-axis or $y$-axis shows the parametric dominance on engine load or $r_p$, respectively. BTE variation was dominantly affected by the engine load, while HC and NOx emissions were dominantly affected by $r_p$. The effect of methanol quantity on NOx emissions at medium engine loads was also evident in this analysis. This analysis showed that $r_p = 0.5$ was the most suitable condition for RCCI combustion mode at all load conditions. At lower engine loads, $r_p = 0.25$ and at higher engine loads, $r_p = 0.75$ could be used to extract benefits of reactivity gradients on the combustion characteristics.

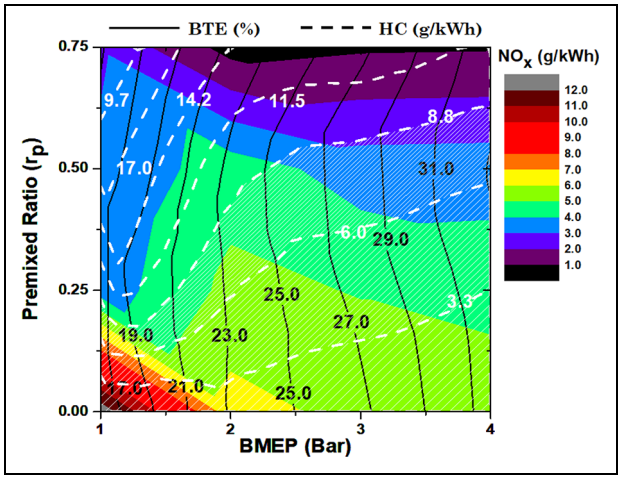


**Figure 8.** Correlation between BTE, HC, and NOx emitted in RCCI combustion mode at different engine loads and premixed ratios.

## *Particulate investigations*

Figure 9 shows the number–size distribution of particles emitted in CI and RCCI combustion modes at different engine loads. In each section, particulate characteristics are discussed, based on their size (mobility diameter, $D_p$), and are further classified as nanoparticles (NP, $D_p < 10\,\text{nm}$), nucleation mode particles (NMP, $10\,\text{nm} < D_p < 50\,\text{nm}$), and accumulation mode particles (AMP, $50\,\text{nm} < D_p < 1000\,\text{nm}$).[43]

Results showed that most particles emitted in CI combustion mode were in the AMP size range; however, particles emitted in the RCCI combustion mode were relatively smaller compared to CI combustion mode. Heterogeneous fuel–air mixing was the main reason for the emission of bigger particles from CI combustion mode, in which soot precursors were generated in the fuel-rich (oxygen-deficient) zones. In RCCI combustion mode, the highly premixed fuel–air mixture was supplied to the combustion chamber, which resulted in a relatively lower number concentration of smaller particles. For both combustion modes, increasing engine load shifted the number–size distribution of particles upward, that is, a higher number of particulate emissions at higher engine loads. The relative dominance of particles in various size ranges (NP, NMP, and AMP) was different in the two combustion modes though. With increasing engine load, the number concentration of AMP increased for both combustion modes; however, the number concentration of NMP decreased. Variations in the number of NPs followed a mixed trend at different engine loads. With increasing engine load, NP first decreased and then increased. A maximum NP concentration was found at BMEP of 4 bar. At maximum engine loads, pyrolysis of lubricating oil due to higher peak in-cylinder temperature may be a possible contributing factor. At all engine loads, particle number concentration decreased with increasing $r_p$.

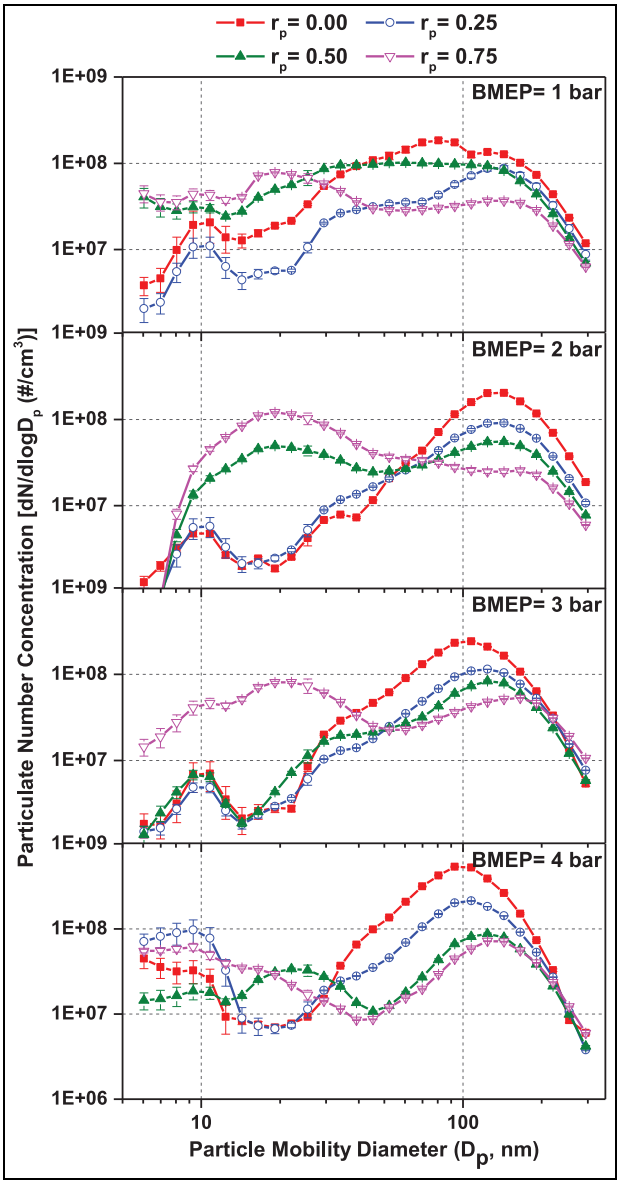


**Figure 9.** Number–size distributions of particulate emitted in RCCI combustion mode at different engine loads and premixed ratios.

However, at lower engine loads, the concentration of smaller particles was higher at higher $r_p$. Relatively lower peak in-cylinder temperature may be a possible reason, which is responsible for generating higher soot precursors due to incomplete combustion. Overall, particle number–size distribution at different $r_p$ and engine loads showed an important trend. Particle number–size distribution in the RCCI combustion mode at higher $r_p$ was similar to spark ignition (SI) combustion mode, especially at lower engine loads, which eventually shifted towards CI combustion mode at higher engine loads. This was due to dominant contribution from the premixed fuel–air mixture at lower engine loads, which dominated over the contributions from direct-injected HRF at higher engine loads.

Figure 10 shows the variations in the number concentration of NPs, NMPs, and AMPs emitted by CI

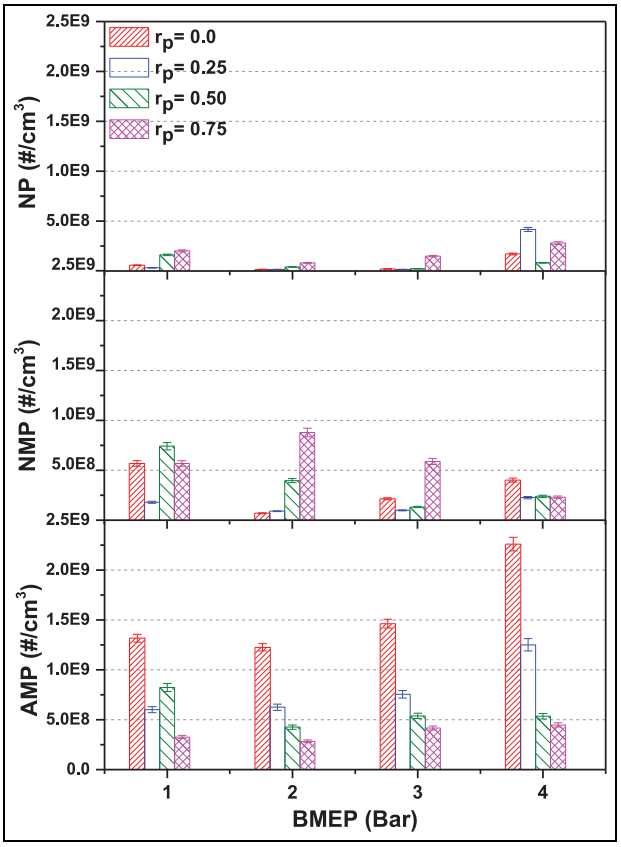


**Figure 10.** Concentration of nanoparticles, nucleation mode particles, and accumulation mode particles emitted in RCCI combustion mode at different engine loads and premixed ratios.

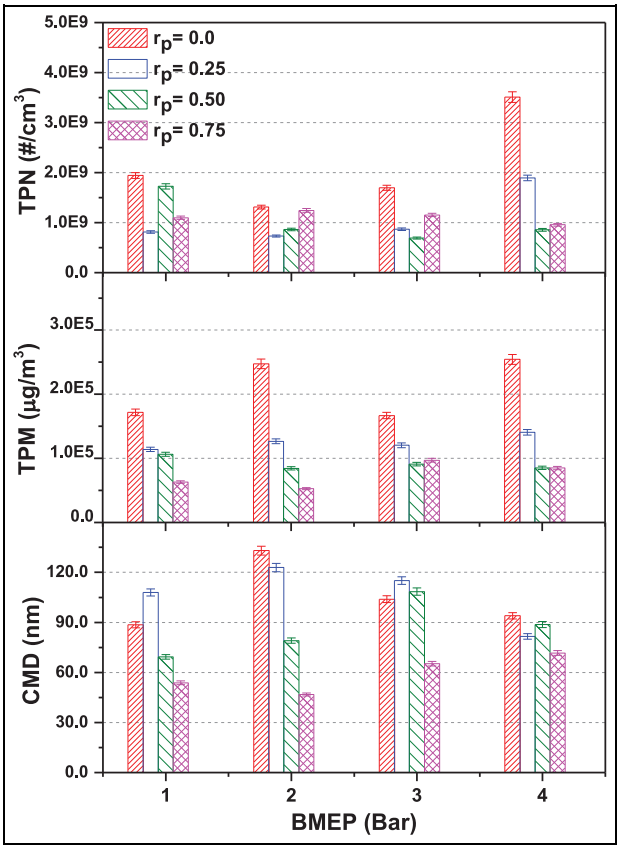


**Figure 11.** Total particle number, total particle mass, and count mean diameter of particles emitted in RCCI combustion mode at different engine loads and premixed ratios.

and RCCI combustion modes at different engine loads and $r_p$.

Results showed that RCCI combustion mode at different engine loads emitted slightly higher NPs compared to CI combustion mode. The number concentration of NPs increased with increasing $r_p$ and $r_p = 0.75$ emitted the maximum NPs. The number concentration of NPs was almost the same at all engine loads and the highest number of NPs were emitted at the maximum engine load (BMEP = 4 bar). NMPs showed a mixed trend for RCCI and CI combustion modes. With increasing engine load, NMP concentration first decreased and then increased. Compared to RCCI combustion mode, CI combustion mode emitted relatively lower NMPs at lower engine loads, which increased at higher engine load (BMEP = 4 bar). In general, it can be concluded that lower $r_p$ of methanol as LRF resulted in a lower number concentration of NMPs at all engine loads; however, higher $r_p$ of methanol as LRF was beneficial for the reduction in NMPs at higher engine loads. Compared to NMPs, the dominating effect of premixed fuel can be clearly seen in the AMPs. At all engine loads, RCCI combustion mode emitted significantly lower AMPs compared to CI combustion mode. AMP number concentration increased with increasing engine load; however, this trend was not very strong in RCCI combustion mode at higher $r_p$. The contribution of LRF in AMP concentration reduction was clearly visible at all engine loads, which showed that increasing $r_p$ resulted in lower AMP concentration. This is the main reason for lower particulate emissions from RCCI combustion mode.

Figure 11 shows the variations in total particle number (TPN), total particulate mass (TPM), and count mean diameter (CMD) of particles emitted in CI and RCCI combustion modes. TPN is the sum of NP, NMP, and AMP number concentrations. In general, TPN increased with increasing engine load. The presence of higher fuel quantity in the combustion chamber was the main reason for higher number of particulate formation. At medium engine loads, higher in-cylinder temperature promoted more soot nuclei formation, leading to higher TPN. The TPN concentration emitted in CI combustion mode was higher compared to RCCI combustion mode. Contribution of fuel-bound oxygen, presence of premixed fuel–air mixture, and sufficient time availability for soot oxidation were the most important factors responsible for this behavior. At all engine loads, increasing $r_p$ showed a mixed trend in TPN variations. Results showed that increasing $r_p$ was more effective at medium engine loads; therefore,

lower $r_p$ was more suitable at lower engine loads and higher $r_p$ was more suitable at medium engine loads.

Similar to TPN, TPM also showed a mixed trend with varying engine loads. At all engine loads, CI combustion mode emitted significantly higher TPM compared to RCCI combustion mode. Compared to TPN, TPM exhibited a direct relationship between $r_p$ and the engine load. At all engine loads, increasing $r_p$ led to lower TPM. This was mainly due to the contribution of fuel-bound oxygen, which oxidized the soot, leading to a reduction in TPM at higher $r_p$. CMD exhibits a superior interpretation of the relationship between engine-out particulate emissions and their adverse health effects. Results showed a mixed trend of CMD at different engine loads and $r_p$. With increasing engine load, CMD of particles first increased and then decreased. CMD of particles emitted in RCCI combustion mode at lower $r_p$ was similar to CI combustion mode; however, RCCI combustion mode at higher $r_p$ emitted relatively smaller particles.

Figure 12 shows the correlation between TPM and NOx emitted in CI and RCCI combustion modes at different engine loads and $r_p$. The importance of RCCI combustion mode can be clearly seen in this analysis, which showed that RCCI combustion mode emitted significantly lower NOx and TPM compared to baseline CI combustion mode. Simultaneous reduction of PM and NOx with increasing $r_p$ is an important observation of this study, which shows that RCCI combustion does not follow the NOx–PM trade-off unlike conventional CI engines. Curran et al.[21] also presented that RCCI combustion reduced NOx and PM emissions simultaneously; however, their investigation a were limited up to lower premixed ratios.

Figure 13 shows the relationship between NOx, TPN, and TPM emitted in the CI and RCCI combustion modes at different engine loads and $r_p$. It can be clearly seen that NOx variation was dominantly controlled by the engine load; however, TPM variation was affected by both, the engine load as well as the $r_p$. At lower engine loads, minimum TPN corresponds to lower $r_p$; whereas at medium engine loads, minimum TPN corresponds to higher $r_p$. At medium engine loads, TPM and NOx were also minimum at higher $r_p$. This analysis depicted that lower NOx and PM emissions could be achieved by using RCCI combustion mode at medium premixed ratio ($r_p$ = 0.50).

## Conclusion

In this experimental study, methanol–diesel-fueled RCCI combustion mode investigations were carried out in a single-cylinder research engine at four engine loads, using three premixed ratios, w.r.t. baseline mineral diesel-fueled CI combustion mode. Combustion results showed that the addition of methanol as LRF significantly improved combustion. RCCI combustion mode

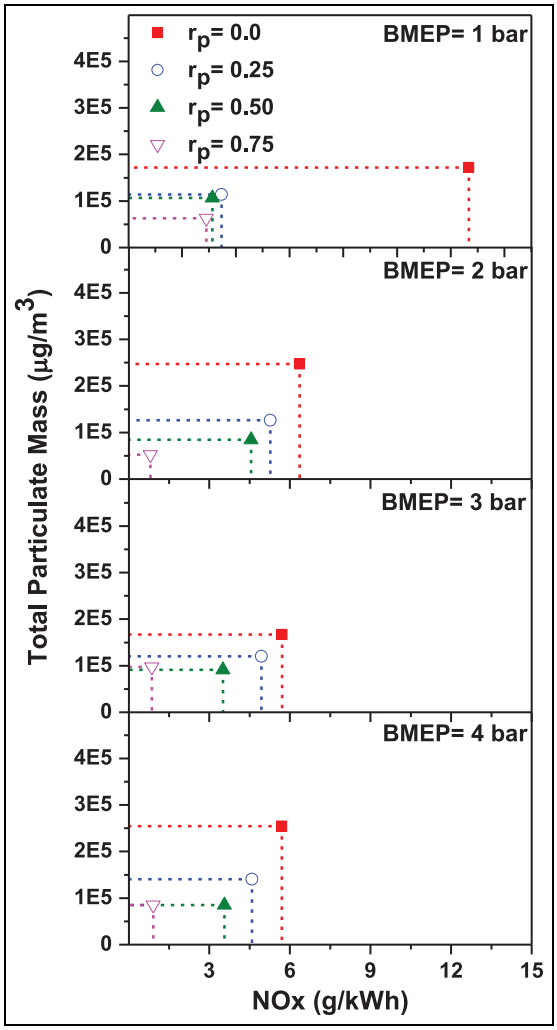


**Figure 12.** Correlation between total particulate mass and NOx emitted in the RCCI combustion mode at different engine loads and premixed ratios.

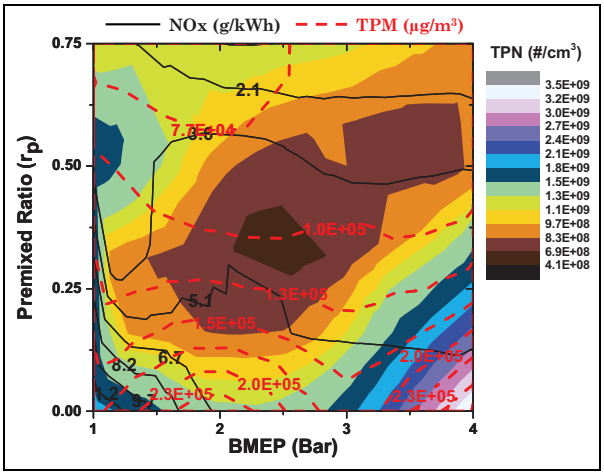


**Figure 13.** Total particle number, total particle mass, and NOx emitted in the RCCI combustion mode at different engine loads and premixed ratios.

was relatively more stable compared to CI combustion mode, especially at medium engine loads. RCCI combustion mode at lower $r_p$ showed higher BTE compared to CI combustion mode. RCCI combustion resulted in significantly lower NOx emissions; however, HC and CO emissions in RCCI combustion mode were relatively higher compared to CI combustion mode. RCCI combustion mode emitted a lesser number of particles compared to CI combustion mode. The similarity of particulate number-size distribution of RCCI combustion mode at higher $r_p$ with SI combustion was another important observation of this study. Particulate characteristics of RCCI combustion mode were dominated by smaller particles (NMPs); however, AMPs were dominant in the CI combustion mode. The NOx–TPM analysis was an important aspect of this study, which exhibited that NOx and PM could be simultaneously reduced by using RCCI combustion mode. Overall, this study demonstrated experimentally that RCCI combustion mode can be easily implemented in modern CI engines to achieve combined benefits of improved engine performance and lower emissions while utilizing potential alternative fuels such as methanol.

## Declaration of conflicting interests

The author(s) declared no potential conflicts of interest with respect to the research, authorship, and/or publication of this article.

## Funding

The author(s) received no financial support for the research, authorship, and/or publication of this article.

## ORCID iD

Avinash Kumar Agarwal https://orcid.org/0000-0002-7777-785X

## References

1. Agarwal AK, Singh AP, Lukose J and Gupta T. Characterization of exhaust particulates from diesel fueled homogenous charge compression ignition combustion engine. *J Aerosol Sci* 2013; 58: 71–85.
2. Agarwal AK, Singh AP, Maurya RK, Shukla PC, Dhar A and Srivastava DK. Combustion characteristics of a common rail direct injection engine using different fuel injection strategies. *Int J Thermal Sci* 2018; 134: 475–484.
3. Shukla PC, Gupta T, Labhasetwar NK, Khobaragade R, Gupta NK and Agarwal AK. Effectiveness of non-noble metal based diesel oxidation catalysts on particle number emissions from diesel and biodiesel exhaust. *Sci Total Environ* 2017; 574: 1512–1520.
4. Pan S, Li X, Han W and Huang Y. An experimental investigation on multi-cylinder RCCI engine fueled with 2-butanol/diesel. *Energy Convers Manag* 2017; 154: 92–101.
5. Nichols RJ. The methanol story: a sustainable fuel for the future. *J Sci Ind Res* 2003; 62: 97–105.
6. Agarwal AK, Sharma N, Singh AP, Kumar V, Satsangi DP and Patel C. Adaptation of methanol–dodecanol–diesel blend in diesel genset engine. *J Energy Resour Technol* 2019; 141(10): 102203.
7. Bromberg L and Cheng WK. Methanol as an alternative transportation fuel in the US: options for sustainable and energy-secure transportation. Sloan Automotive Laboratory, Massachusetts Institute of Technology, Cambridge, MA, 2010.
8. Anand K, Sharma RP and Mehta PS. Experimental investigations on combustion, performance and emissions characteristics of neat karanji biodiesel and its methanol blend in a diesel engine. *Biomass Bioenergy* 2011; 35(1): 533–541.
9. Agarwal AK, Karare H and Dhar A. Combustion, performance, emissions and particulate characterization of a methanol–gasoline blend (gasohol) fuelled medium duty spark ignition transportation engine. *Fuel Process Technol* 2014; 121: 16–24.
10. Rakopoulos DC, Rakopoulos CD, Hountalas DT, Kakaras EC, Giakoumis EG and Papagiannakis RG. Investigation of the performance and emissions of bus engine operating on butanol/diesel fuel blends. *Fuel* 2010; 89: 2781–2790.
11. Singh AP, Sharma N, Satsangi DP, Kumar V and Agarwal AK. Reactivity-controlled compression ignition combustion using alcohols. In: Agarwal AK, Gupta JG, Sharma N and Singh AP (eds) *Advanced engine diagnostics*. Singapore: Springer, 2019, pp.9–28.
12. Agarwal AK, Singh AP and Maurya RK. Evolution, challenges and path forward for low temperature combustion engines. *Progr Energy Combust Sci* 2017; 61: 1–56.
13. Yao M, Zheng Z and Liu H. Progress and recent trends in homogeneous charge compression ignition (HCCI) engines. *Progr Energy Combust Sci* 2009; 35: 398–437.
14. Lu X, Han D and Huang Z. Fuel design and management for the control of advanced compression-ignition combustion modes. *Progr Energy Combust Sci* 2011; 37: 741–783.
15. Singh AP, Bajpai N and Agarwal AK. Combustion mode switching characteristics of a medium duty engine operated in compression ignition/PCCI combustion modes. *J Energy Resour Technol* 2018; 140(9): 092201.
16. Singh AP and Agarwal AK. CI/PCCI combustion mode switching of diesohol fuelled production engine. SAE technical paper 2017-01-0738, 2017.
17. Kokjohn SL, Hanson RM, Splitter DA and Reitz RD. Fuel reactivity controlled compression ignition (RCCI): a pathway to controlled high-efficiency clean combustion. *Int J Engine Res* 2011; 12: 209–226.
18. Kokjohn SL, Hanson RM, Splitter DA and Reitz RD. Experiments and modeling of dual-fuel HCCI and PCCI combustion using in-cylinder fuel blending. SAE technical paper 2009-01-2647, 2009.
19. Kokjohn S, Hanson R, Splitter D, Kaddatz J and Reitz R. Fuel reactivity controlled compression ignition (RCCI) combustion in light- and heavy-duty engines. *SAE Int J Engines* 2011; 4(1): 360–374.
20. Zhou DZ, Yang WM, An H and Li J. Application of CFD-chemical kinetics approach in detecting RCCI engine knocking fuelled with biodiesel/methanol. *Appl Energy* 2015; 145: 255–264.

21. Curran S, Prikhodko V, Cho K, Sluder CS, Parks J, Wagner R, et al. In-cylinder fuel blending of gasoline/diesel for improved efficiency and lowest possible emissions on a multi-cylinder light-duty diesel engine. SAE technical paper 2010-01-2206, 2010.
22. Curran SJ, Hanson RM and Wagner RM. Reactivity controlled compression ignition combustion on a multi-cylinder light-duty diesel engine. *Int J Engine Res* 2012; 13(3): 216–225.
23. Dempsey AB and Reitz RD. Computational optimization of reactivity controlled compression ignition in a heavy-duty engine with ultra low compression ratio. *SAE Int J Engines* 2011; 4: 2222–2239.
24. Splitter D, Reitz R and Hanson R. High efficiency low emissions RCCI combustion by use of a fuel additive. *SAE Int J Fuels Lubr* 2010; 3(2):742-756.
25. Hanson RM, Kokjohn SL, Splitter DA and Reitz RD. An experimental investigation of fuel reactivity controlled PCCI combustion in a heavy-duty engine. SAE technical paper 2010-01-0864, 2010.
26. Nieman D, Dempsey A and Reitz R. Heavy-duty RCCI operation using natural gas and diesel. *SAE Int J Engines* 2012; 5(2): 270–285.
27. Zheng Z, Li C, Liu H, Zhang Y, Zhong X and Yao M. Experimental study on diesel conventional and low temperature combustion by fueling four isomers of butanol. *Fuel* 2015; 141: 109–119.
28. Hanson R, Kokjohn S, Splitter D and Reitz R. An experimental investigation of fuel reactivity controlled PCCI combustion in a heavy-duty engine. *SAE Int J Engines* 2010; 3(1): 700–716.
29. Anderson JE, Kramer U, Mueller SA and Wallington TJ. Octane numbers of ethanol− and methanol−gasoline blends estimated from molar concentrations. *Energy Fuels* 2010; 24(12): 6576–6585.
30. Dempsey AB, Walker NR and Reitz R. Effect of cetane improvers on gasoline, ethanol, and methanol reactivity and the implications for RCCI combustion. *SAE Int J Fuels Lubr* 2013; 6(1): 170–187.
31. Li Y, Jia M, Chang Y, Liu Y, Xie M, Wang T, et al. Parametric study and optimization of a RCCI (reactivity controlled compression ignition) engine fueled with methanol and diesel. *Energy* 2014; 65(11): 319–332.
32. Singh AP and Agarwal AK. Diesoline, diesohol, and diesosene fuelled HCCI engine development. *J Energy Resour Technol* 2016; 138: 052212-1.
33. Singh AP, Pal P and Agarwal AK. Comparative particulate characteristics of hydrogen CNG, HCNG, gasoline and diesel-fuelled engines. *Fuel* 2016; 185(1): 491–499.
34. Singh AP, Pal P, Gupta NK and Agarwal AK. Particulate emissions from laser ignited and spark ignited hydrogen fuelled engines. *Int J Hydrog Energy* 2017; 42(24): 15956–15965.
35. Rassweiler G and Withrow L. Motion pictures of engine flames correlated with pressure cards. *SAE technical paper* 380139, 1938.
36. Jain A, Singh AP and Agarwal AK. Effect of fuel injection parameters on combustion stability and emissions of a mineral diesel fueled partially premixed charge compression ignition (PCCI) engine. *Appl Energy* 2017; 190: 658–669.
37. Heywood JB. *Internal combustion engine fundamentals*. New York: McGraw-Hill Book, 1988.
38. Paykani A, Kakaee A, Rahnama P and Reitz RD. Progress and recent trends in reactivity-controlled compression ignition engines. *Int J Eng Res* 2016; 17(5): 481–524.
39. Jain A, Singh AP and Agarwal AK. Effect of split fuel injection and EGR on NOx and PM emission reduction in a low temperature combustion (LTC) mode diesel engine. *Energy* 2017; 122: 249–264.
40. Agarwal AK, Agarwal A and Singh AP. Time resolved in-situ biodiesel combustion visualization using engine endoscopy. *Measurement* 2015; 69: 236–249.
41. Han Z, Li B, Tian W, Xia Q and Leng S. Influence of coupling action of oxygenated fuel and gas circuit oxygen on hydrocarbons formation in diesel engine. *Energy* 2019; 173: 196–206.
42. Indian standard IS: 14273, Automotive vehicles—exhaust emissions—gaseous pollutants from vehicles fitted with compression ignition engines—method of measurement, Bureau of Indian Standards, New Delhi, India, 1999.
43. Engine Exhaust Particle Sizer™ Spectrometer Model 3090. Operation and Service Manual, TSI, USA, March 2009.